

Hyperspherical Graph Representation Learning via Adaptive Neighbor-Mean Alignment and Uniformity [★]

Rui Chen^{a,b}, Junjun Guo^{a,b}, Hongbin Wang^{a,b}, Yan Xiang^{a,b}, Yantuan Xian^{a,b,*},
Zhengtao Yu^{a,b,*}

^a*Faculty of Information Engineering and Automation, Kunming University of Science and Technology, , Kunming, 650500, Yunnan, China*

^b*Yunnan Key Laboratory of Artificial Intelligence, Kunming University of Science and Technology, , Kunming, 650500, Yunnan, China*

Abstract

Graph representation learning (GRL) aims to encode structural and semantic dependencies of graph-structured data into low-dimensional embeddings. However, existing GRL methods often rely on surrogate contrastive objectives or mutual information maximization, which typically demand complex architectures, negative sampling strategies, and sensitive hyperparameter tuning. These design choices may induce over-smoothing, over-squashing, and training instability. In this work, we propose **HyperGRL**, a unified framework for **Hyperspherical Graph Representation Learning** via Adaptive Neighbor-Mean Alignment and Uniformity, which embeds nodes on a unit hypersphere through two adversarially coupled objectives: **Neighbor-Mean Alignment** and **Sampling-Free Uniformity**. The alignment objective uses the mean representation of each node's local neighborhood to construct semantically grounded, stable targets that capture shared structural and feature patterns. The uniformity objective formulates dispersion via an ℓ_2 -based hyperspherical regularization, encouraging globally uniform embedding distributions while preserving discriminative information. To further stabilize training, we introduce an **Entropy-Guided Adaptive Balancing** mechanism that dynamically regulates the interplay between alignment and uniformity without requiring manual tuning.

[★]Submitted to Pattern Recognition.

^{*}Corresponding author.

Email addresses: chen_rui@stu.kust.edu.cn (Rui Chen), 20170039@kust.edu.cn (Junjun Guo), whbin2013@kust.edu.cn (Hongbin Wang), yanx@kust.edu.cn (Yan Xiang), xianyt@kust.edu.cn (Yantuan Xian), yuzt@kust.edu.cn (Zhengtao Yu)

Extensive experiments on node classification, node clustering, and link prediction tasks demonstrate that **HyperGRL** delivers superior representation quality and generalization across diverse graph structures, achieving average improvements of 1.49%, 0.86%, and 0.74% over the strongest existing methods, respectively. These findings highlight the effectiveness of geometrically grounded, sampling-free contrastive objectives for graph representation learning.

Keywords: Graph Representation Learning, Contractive Learning, Neighbor-Mean Alignment, Negative-Free Uniformity, Graph Neural Networks

1. Introduction

Graph representation learning (GRL) has emerged as a fundamental paradigm for learning expressive and transferable node embeddings from graph-structured data. Among its various approaches, Graph Contrastive Learning (GCL) has become a cornerstone framework that leverages contrastive objectives to capture both structural and semantic dependencies without explicit supervision [1, 2, 3]. Broadly, existing methods can be categorized into three major families: *InfoNCE-based* approaches, which perform instance-level discrimination by distinguishing each node (or subgraph) from all others via noise-contrastive estimation [1, 4]; *DGI-like* methods, which perform group-level discrimination by maximizing the mutual information between local (node) and global (graph-level) representations [2, 5], and *BGRL-like or bootstrapping* methods, which replace explicit negatives with momentum-updated target encoders, stabilizing training through self-distillation [3, 6].

Despite differences in their architectures and training objectives, all these approaches can be unified under the *alignment-uniformity principle* [7], which is firstly introduced for non-graph contrastive representation learning. This principle asserts that effective representations must simultaneously (i) align semantically or structurally related samples in the embedding space and (ii) ensure uniformity across the manifold (typically a unit hypersphere) to avoid representational collapse and maintain discriminability. From this perspective, InfoNCE-based methods [1, 4, 8, 9] explicitly enforce both aspects through attraction between positive pairs and repulsion among sampled negatives. DGI-

like methods [2, 5, 10] achieve a similar outcome implicitly by maximizing mutual information, with the global discriminator promoting broad coverage of the feature space. Bootstrapped methods[3, 6, 11, 12], such as BGRL [3] and BYOL[6], induce uniformity indirectly via predictor asymmetry and normalization constraints that prevent collapse. Thus, the alignment-uniformity framework offers a cohesive geometric lens on the varied landscape of GCL models, elucidating their common inductive biases and optimization behaviors.

However, translating the alignment-uniformity principle to graph remains nontrivial. Graph structures exhibit irregular connectivity, high-degree heterogeneity, and topology-dependent semantics, making it difficult to generate reliable alignment targets with feature argumentation. Existing GCL methods often rely on **graph augmentations** (e.g., feature masking, edge perturbation, subgraph sampling) [12, 13] or **auxiliary encoders and predictors** [11, 14], such as dual-encoder architectures, to construct positive pairs. While these designs provide useful supervision, they are typically heuristic, computationally costly, and prone to unstable optimization due to the **absence of explicit, model-internal alignment anchors**. Likewise, uniformity is usually enforced via **sampling-based negatives**, which may introduce noise, bias, or redundant comparisons that fail to guarantee global coverage of the hypersphere. Moreover, many GCL frameworks suffer from **hyperparameter sensitivity**, requiring dataset-specific adjustment of the weighting between alignment and uniformity losses to stabilize training and prevent collapse [7, 15]. This sensitivity undermines robustness, scalability, and reproducibility, particularly on heterogeneous or large-scale graphs.

To address these limitations, we propose **HyperGRL**, a hyperspherical graph representation learning framework that integrates adaptive neighbor-mean alignment and sampling-free uniformity for effective node representation learning. The core design choices of HyperGRL are threefold: (1) Neighbor-Mean Alignment. Instead of constructing positive views (or alignment target) through augmentations or auxiliary encoders, we use the mean vector of a node’s neighborhood as an explicit, stable alignment target. The Neighbor-Mean captures intrinsic local structure and can be recursively extended to higher-order neighborhoods, enabling progressively broader and smoother structural alignment. (2) Hyperspherical Uniformity. Rather than relying on sampled negatives,

we impose global uniformity through a squared ℓ_2 -norm that encourages embeddings to spread uniformly across the unit hypersphere. This drives the encoder to fully utilize the spherical manifold, yielding diverse and well-separated representations without explicit negative pairs. (3) Entropy-Guided Adaptive Balancing. To alleviate brittle hyperparameter tuning between alignment and uniformity, we introduce an entropy-driven adaptive weighting scheme that dynamically adjusts weight for uniformity loss during training. When embeddings become overly concentrated (low entropy), the weight is increased to emphasizes uniformity otherwise when the weight is decreased.

In summary, our main contributions are as follows:

- (1) A novel, effective alignment-uniformity framework for graph representation learning. The proposed neighbor-mean alignment mechanism provide a consistent, stable alignment target, without auxiliary encoders or positive pair sampling. The proposed ℓ_2 -norm-based uniformity loss enforces global uniformity on the unit hyperspherical without sampled negatives.
- (2) An entropy-guided adaptive balancing mechanism that automatically balances alignment and uniformity, substantially reducing the need for manual hyperparameter tuning.
- (3) Extensive empirical validation of downstream tasks on public graph datasets showing that HyperGRL produces more discriminative, stable, and generalizable node representations across diverse graph datasets and tasks.

2. Related Work

2.1. *Self-supervised Graph Representation Learning*

Self-supervised graph representation learning is a dominant approach that exploits large amounts of unlabeled data by employing carefully designed pretext tasks to learn expressive representations. Early approaches primarily adopted reconstruction-based objectives, such as masked feature modeling or graph autoencoders, to capture both attribute and structural dependencies [16, 17]. Subsequent methods shifted toward predictive or clustering-based tasks to provide richer supervisory signals [5, 18]. More recently, UMGRL [19] extends this line by maximizing coding-rate reduction to jointly

enhance the diversity, discrimination, and consistency of representations on multiplex graphs. Despite these advances, existing approaches remain limited by their reliance on reconstruction or handcrafted objectives, which has motivated the development of contrastive paradigms that enforce consistency across augmented views.

2.2. *Graph Contrastive Learning*

Among self-supervised approaches, Graph Contrastive Learning (GCL) focuses on maximizing agreement between related nodes or subgraphs while distinguishing unrelated ones. Early work such as DGI [2] operationalizes this idea by maximizing mutual information between local node embeddings and a global summary vector, thereby encouraging nodes to capture graph-level structural signals. GRACE [1] introduces graph augmentations such as edge perturbation and feature masking, and enforces consistency between augmented views of the same graph via a contrastive loss. At the graph level, DualGCL [20] adopts a dual-channel contrastive framework that jointly captures local and global information, reducing the need for handcrafted augmentations. Recent approaches like BGRL [14] further simplify the paradigm by eliminating explicit negative samples through bootstrap learning. Despite their empirical success, these methods still face over-compression and collapse, highlighting the need for geometric priors to better regulate embedding distributions.

2.3. *Hyperspherical Representation Learning*

Hyperspherical representation learning enhances embedding quality by exploiting the geometry of the unit hypersphere. Methods based on the von Mises–Fisher (vMF) distribution, such as HCAN [21] and DAGC [22], model node embeddings as directional distributions on the hypersphere, allowing the representation of both concentration and uncertainty while better capturing directional similarity. HPNC [23] further enforces inter-cluster separability by uniformly distributing cluster prototypes on the hypersphere, providing explicit geometric regularization that mitigates representation collapse. In parallel, the alignment–uniformity framework [7] and SGRL [24] reveal that balancing attraction and dispersion is crucial for contrastive objectives. However, prior studies often treat dispersion and cohesion separately, whereas our approach unifies them under

a neighbor mean guided framework, providing a geometrically grounded solution for robust and discriminative graph representations.

3. Preliminary

3.1. Problem Statement

Consider a graph $\mathcal{G} = (\mathcal{V}, \mathcal{E})$, where \mathcal{V} denotes the node set, and $\mathcal{E} \subseteq \mathcal{V} \times \mathcal{V}$ represents the edge set. Let $N = |\mathcal{V}|$ denote the number of nodes. The graph is associated with an adjacency matrix $\mathbf{A} \in \mathbb{R}^{N \times N}$ and a node feature matrix $\mathbf{X} \in \mathbb{R}^{N \times F}$, where F is the feature dimension. Our objective is to learn a graph encoder $f_\theta(\cdot)$ that maps the structural and attribute information of \mathcal{G} into a latent space, yielding node embeddings $\mathbf{H} = f_\theta(\mathbf{A}, \mathbf{X}) \in \mathbb{R}^{N \times d}$, where d denotes the embedding dimension. Importantly, the learning process is conducted in a self-supervised manner, i.e., without relying on any label information.

3.2. Hypersphere Graph Node Representation

Compared with Euclidean embeddings, spherical graph node representations exhibit several significant advantages for graph representation learning. First, the normalization constraint ensures all embeddings lie on a unit hypersphere, eliminating scale variations and making the representations inherently comparable. Second, similarity is naturally measured by cosine similarity or angular distance, which is well aligned with contrastive learning objectives. Third, the hyperspherical constraint acts as an implicit geometric regularization, promoting more discriminative and robust embeddings. In addition, spherical representations naturally connect with probabilistic modeling on manifolds, such as the von Mises–Fisher distribution, which further enhances their theoretical interpretability.

Formally, we consider embedding nodes into a $(d - 1)$ -dimensional unit hypersphere defined as

$$\mathbb{S}^{d-1} = \{\mathbf{h} \in \mathbb{R}^d : \|\mathbf{h}\|_2 = 1\}. \quad (1)$$

Given a graph encoder $f_\theta(\cdot)$, the initial node embeddings are obtained as $\mathbf{H} = f_\theta(\mathbf{A}, \mathbf{X}) \in \mathbb{R}^{N \times d}$. To enforce the spherical constraint, each node embedding is projected

onto the hypersphere by

$$\mathbf{z}_i = \text{normalize}(\mathbf{h}_i) = \frac{\mathbf{h}_i}{\|\mathbf{h}_i\|_2}, \quad \forall i \in \{1, 2, \dots, N\}, \quad (2)$$

where \mathbf{h}_i is the i -th row of \mathbf{H} . The normalized embeddings $\mathbf{Z} = [\mathbf{z}_1; \mathbf{z}_2; \dots; \mathbf{z}_N]$ therefore lie strictly on the hypersphere and serve as the foundation representations of our proposed framework.

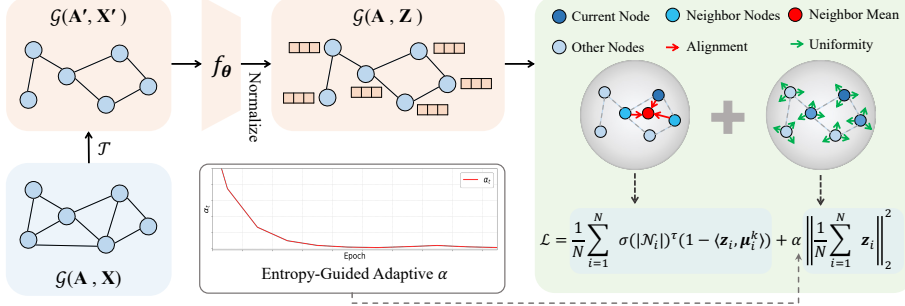


Figure 1: Overview of HyperGRL. Given a graph $\mathcal{G}(\mathbf{A}, \mathbf{X})$, a graph augmentation \mathcal{T} produces an augmented graph $\mathcal{G}(\mathbf{A}', \mathbf{X}')$. This augmented graph is then encoded by a GNN f_θ to generate node representations \mathbf{H} . These representations are subsequently normalized onto a hyperspherical space to yield \mathbf{Z} , where training is driven by two complementary objectives: the *Neighbor-Mean Alignment* loss $\mathcal{L}_{\text{align}}$, which pulls each node toward the mean representation of its neighbors, and the *Uniformity* loss $\mathcal{L}_{\text{unif}}$, which encourages the node representations to be uniformly distributed across the unit hypersphere.

4. Hyperspherical Graph Representation Learning via Adaptive Neighbor-Mean Alignment and Uniformity

This section introduces the proposed HyperGRL framework. Section 4.1 describes the graph neural encoder that projects node features into a normalized hyperspherical space. Section 4.2 details the *Neighbor-Mean Alignment* mechanism, which establishes stable and semantically consistent alignment targets for local structural learning. Section 4.3 introduces the *Uniformity Loss*, which enforces global uniformity and mitigates representation collapse by encouraging embeddings to disperse uniformly over the hypersphere. Section 4.4 further presents the *Adaptive Balancing Objective*

Function, incorporating an entropy-guided weighting strategy that dynamically adjusts the trade-off between alignment and uniformity through entropy-based self-calibration.

4.1. Graph Neural Network Encoder

We adopt a graph neural network (GNN) as the backbone encoder to jointly capture the structural dependencies and attribute semantics of the input graph. Formally, given an adjacency matrix \mathbf{A} and a feature matrix \mathbf{X} , the encoder $f_\theta(\cdot)$ maps each node to a latent representation space as

$$\mathbf{H} = f_\theta(\mathbf{A}, \mathbf{X}) = \text{GNN}(\mathbf{A}, \mathbf{X}) \in \mathbb{R}^{N \times d}. \quad (3)$$

To improve the discriminative power and numerical stability of the learned representations, we further constrain them to lie on a unit hypersphere by applying ℓ_2 normalization:

$$\mathbf{Z} = \text{normalize}(\mathbf{H}) \in \mathbb{S}^{N \times (d-1)}, \quad (4)$$

where \mathbf{Z} denotes the hypersphere node representations.

To enhance representation robustness and facilitate contrastive learning, we construct an augmented view of the input graph at each training iteration. Following established practice [14], we employ two complementary yet lightweight augmentation operations *feature masking* and *edge perturbation* to define the augmentation function \mathcal{T} . Specifically, given a graph $\mathcal{G} = (\mathbf{A}, \mathbf{X})$, we stochastically drop a subset of edges and feature dimensions according to Bernoulli distributions:

$$\begin{aligned} \mathbf{E}' &= \text{Bernoulli}(\mathbf{E}, 1 - p_e), \quad 0 < p_e < 1, \\ \mathbf{X}' &= \text{Bernoulli}(\mathbf{X}, 1 - p_x), \quad 0 < p_x < 1, \end{aligned} \quad (5)$$

where p_e and p_x represent the drop ratios for edges and feature dimensions, respectively. The perturbed adjacency matrix \mathbf{A}' and feature matrix \mathbf{X}' are subsequently fed into the encoder, encouraging the model to learn invariances to both structural noise and attribute corruption while preserving task-relevant information.

In this work, we employ Graph Transformer [25] as the encoder for graph representation learning. However, HyperGRL is model-agnostic and can be easily implemented with other GNN architectures such as GCN [26], GAT [27], and GraphSAGE [28].

4.2. Neighbor-Mean Alignment Loss

We define the alignment target μ_i for a node i as the normalized mean of its neighbors' representations $\{z_j\}_{j \in \mathcal{N}_i}$, which named 1-order mean alignment vectors,

$$\tilde{\mu}_i = \frac{1}{|\mathcal{N}_i|} \sum_{j \in \mathcal{N}(i)} z_j, \quad \mu_i = \text{normalize}(\tilde{\mu}_i). \quad (6)$$

To enhance the clusterability and the robustness of the alignment target, we further introduce a k -order mean by recursively averaging the $(k-1)$ -order alignment vectors of the neighbors:

$$\tilde{\mu}_i^k = \frac{1}{|\mathcal{N}_i|} \sum_{j \in \mathcal{N}(i)} \mu_j^{k-1}, \quad \mu_i^k = \text{normalize}(\tilde{\mu}_i^k). \quad (7)$$

To enhance representation consistency among structurally similar or densely connected nodes, we introduce an *alignment loss* that encourages each node to align its representation with the k -order mean of its neighbors:

$$\mathcal{L}_{\text{align}} = \frac{1}{N} \sum_{i=1}^N \sigma(|\mathcal{N}_i|)^{\tau} (1 - \langle z_i, \mu_i^k \rangle), \quad (8)$$

where the inner product $\langle \cdot, \cdot \rangle$ denotes the cosine similarity on the unit hypersphere, $\sigma(\cdot)$ is the sigmoid function. The hyperparameter τ controls the sensitivity of the per-node weighting by the node's degree $|\mathcal{N}_i|$, which adaptively emphasizes or de-emphasizes the alignment contribution of each node based on its local density.

We argue that the neighbor mean serves as an effective and inherently robust alignment target within the representation space. From a structural perspective, when a node resides in a densely connected subgraph, the aggregation of its neighbors yields a highly coherent mean vector, thereby enforcing local smoothness and promoting convergence of strongly associated nodes toward similar representations. Conversely, when a node is located in a sparse or weakly connected region, the resulting neighbor mean becomes more dispersed. This adaptive property prevents over-compression of representations and preserves the expressive capacity of the latent space, enabling the model to maintain a balance between local consistency and global discriminability across heterogeneous graph topologies.

4.3. Uniformity Loss

While the alignment loss encourages cohesion within local neighborhoods at various hierarchical levels, excessive contraction can lead to representation collapse, where embeddings converge toward a low-dimensional subspace or even a single point on the hypersphere. To counteract this, we incorporate a uniformity-promoting mechanism that enforces dispersion across the entire representation space, thereby maintaining a balanced and uniform distribution of embeddings on the unit hypersphere.

Formally, given the normalized node embeddings $\{z_i\}_{i=1}^N$, we define the *uniformity loss* as the squared ℓ_2 -norm of their empirical mean:

$$\mathcal{L}_{\text{unif}} = \left\| \frac{1}{N} \sum_{i=1}^N z_i \right\|_2^2. \quad (9)$$

This loss directly penalizes deviations from a zero-centered distribution, as a uniform spread of unit vectors on the hypersphere implies that their vector average approaches the origin in high dimensions. By minimizing $\mathcal{L}_{\text{unif}}$, the model is encouraged to push embeddings apart in a balanced manner, mitigating over-smoothing and enhancing the overall discriminability and information capacity of the latent space. This approach aligns with established principles in hyperspherical representation learning, where centering the embeddings promotes maximal entropy and prevents collapse [7].

4.4. Adaptive Balancing Objective

We construct the final training objective by jointly optimizing the adversarial interplay between the alignment and uniformity losses:

$$\mathcal{L} = \mathcal{L}_{\text{align}}^k + \alpha \mathcal{L}_{\text{unif}}, \quad (10)$$

where $\mathcal{L}_{\text{align}}^k$ denotes the k -order neighbor mean alignment loss, and α is a hyperparameter that balances the contributions of the uniformity and alignment terms.

While the static hyperparameter α in Equation (10) provides a straightforward means to balance the contributions of $\mathcal{L}_{\text{align}}^k$ and $\mathcal{L}_{\text{unif}}$, it may not optimally adapt to varying training dynamics or heterogeneous graph structures. For instance, in early training stages or on sparse graphs, excessive uniformity could disrupt local cohesion, whereas

in later stages or dense subgraphs, over-alignment risks representational collapse. To address this, we introduce an **Entropy-Guided Adaptive Balancing (EGAB)** mechanism that dynamically adjusts α based on node representations $\{z_i^k\}_{i=1}^N$. This approach leverages entropy as a proxy for representational diversity on the hypersphere, ensuring a responsive trade-off that promotes both convergence stability and generalization.

4.4.1. Entropy Estimation

Direct entropy computation on high-dimensional embeddings is intractable, so we employ an efficient proxy derived from the collapse metric C , which is equal to *Uniformity Loss*, Eq.9. It measures the squared norm of the average mean vector. For uniformly distributed vectors on a high-dimensional hypersphere, $C \approx 0$, indicating high entropy and maximal dispersion. Conversely, $C \approx 1$ signals collapse toward a single direction, reflecting low entropy.

We map C to a pseudo-entropy H_{proxy} :

$$H_{\text{proxy}} = -\log(C + \epsilon), \quad (11)$$

where $\epsilon = 10^{-6}$ prevents numerical instability. This proxy inversely correlates with collapse, aligning with uniformity principles in hyperspherical representation.

4.4.2. Adaptive Weighting Rule

At the end of each training epoch t , we update $\hat{\alpha}_t$ relative to a target entropy H_{target} , which approximated as $\log(d)$ for embedding dimension d :

$$\hat{\alpha}_t = \alpha_{\min} + (\alpha_{\max} - \alpha_{\min}) \cdot \sigma\left(\beta \left(\frac{H_{\text{target}} - H_{\text{proxy},t}}{H_{\text{target}}}\right)\right), \quad (12)$$

where $\sigma(\cdot)$ is the sigmoid function, $\beta > 0$ controls transition sharpness, and $\alpha_{\min}, \alpha_{\max}$ bound the range. When $H_{\text{proxy},t} < H_{\text{target}}$, it means low diversity, potential collapse, α_t increases to emphasize uniformity. When $H_{\text{proxy},t} \approx H_{\text{target}}$, it means balanced diversity, α_t decreases, prioritizing alignment.

To mitigate oscillations, we apply an exponential moving average, with $\gamma = 0.1$:

$$\alpha_t \leftarrow (1 - \gamma)\alpha_{t-1} + \gamma\hat{\alpha}_t. \quad (13)$$

5. Experiments

5.1. Experimental Setup

5.1.1. Datasets

We conduct experiments on eight widely used benchmark datasets spanning diverse domains and graph scales, providing a comprehensive and reliable basis for evaluation. Specifically, the Cora, CiteSeer, and PubMed citation networks [26] are standard benchmarks where nodes represent papers and edges represent citation links. WikiCS [29] is a Wikipedia-based network that contains articles as nodes and hyperlinks as edges, with topic labels for classification. Amazon-Computers and Amazon-Photo are product co-purchase networks, while Coauthor-CS and Coauthor-Physics are academic co-authorship networks [30], where nodes correspond to products or authors and edges represent co-purchase or collaboration relations. We summarize the dataset statistics in Table 1 for reference. The average degree is computed as $2\frac{|\mathcal{E}|}{|\mathcal{V}|}$, where $|\mathcal{E}|$ and $|\mathcal{V}|$ denote the number of edges and the number of nodes, respectively.

Table 1: Statistics of the used datasets.

Dataset	Nodes	Edges	Features	Classes	Avg. Deg.
Cora	2,708	5,278	1,433	7	3.90
CiteSeer	3,327	4,522	3,703	6	2.72
PubMed	19,717	44,324	500	3	4.50
WikiCS	11,701	216,123	300	10	36.93
Amz.-Comp.	13,752	245,861	767	10	35.75
Amz.-Photo	7,650	119,081	745	8	31.13
Co.-CS	18,333	81,894	6,805	15	8.94
Co.-Physics	34,493	247,962	8,415	5	14.38

5.1.2. Baselines

We compare HyperGRL with a wide range of baseline methods across three tasks—node classification, node clustering, and link prediction—to systematically assess its ability to learn discriminative and generalizable node representations.

For node classification: (1) *Supervised learning methods*: MLP and GCN [26]; (2) *Classical graph embedding methods*: DeepWalk [31] and Node2Vec [32]; (3) *Graph contrastive learning methods*: including the mainstream baselines DGI [2], GRACE [1], and BGRL [14], along with VGAE [16], GMI [33], MVGRL [5], GCA [8], CCA-SSG [34], SUGRL [35], SGCL [12], and SGRL [24].

For node clustering: DGI [2], BGRL [14], and SGRL [24].

For link prediction: (1) *Embedding methods*: MF [36], MLP and Node2Vec [32]; (2) *GNN-based methods*: GCN [26], GAT [27], SAGE [28] and VGAE [16]; (3) *Advanced GNNs for link prediction (GNN4LP)*: SEAL [37], BUDDY [38], NBFNet [39], Neo-GNN [40], PEG [41], NCN and NCNC [42].

5.1.3. Evaluation

For a fair and reproducible comparison, we evaluate HyperGRL across three representative downstream tasks: node classification, node clustering, and link prediction. All reported results are averaged over twenty independent runs with different random splits and model initializations to ensure statistical robustness.

For node classification tasks, we followed the linear classification evaluation protocol from [3]. Specifically, the graph encoder is first pre-trained in a self-supervised manner to obtain node representations, upon which a Q^2 -regularized logistic regression classifier is trained for downstream node classification. The classification performance is reported in terms of accuracy (%).

For node clustering tasks, we followed the evaluation setup from [11], where k -means clustering is performed on the pre-trained node representations. The quality of the clustering is assessed using Normalized Mutual Information (NMI).

For link prediction tasks, we adhered to the evaluation protocol outlined in [43], where the embeddings of node pairs are concatenated and fed into a two-layer MLP decoder to predict missing edges. The performance of the link prediction task is measured using the Area Under the ROC Curve (AUC).

5.1.4. Implementation Details

We implement HyperGRL using the PyTorch Geometric library, adopting the TransformerConv layer with SiLU activation as the encoder backbone. All models are trained with the Adam optimizer (learning rate 10^{-3} , weight decay 10^{-5}) for up to 1500 epochs, with early stopping applied based on the minimum training loss. The embedding dimension is set to 1024, with the hyperparameters fixed as $k = 1$, $\tau = 5$, $p_e = 0.8$, and $p_x = 0.1$ unless otherwise stated. All experiments are conducted on a single NVIDIA RTX 4090 GPU. During downstream evaluation, the encoder parameters remain frozen to ensure a fair and consistent assessment of the learned representations.

Beyond the aforementioned fixed parameters, the target entropy H_{target} is determined based on the sparsity of each graph. Specifically, for relatively sparse graphs—such as Cora, CiteSeer, PubMed, Coauthor-CS, and Coauthor-Physics—we set $H_{\text{target}} = 1.5$. In contrast, for denser graphs including WikiCS, Amazon-Computers, and Amazon-Photo, a higher target entropy of $H_{\text{target}} = 2.0$ is adopted to accommodate their richer structural and attribute information, thereby alleviating potential over-smoothing effects. The categorization of sparse versus dense graphs follows the average degree statistics summarized in Table 1.

5.2. Node Classification

Table 2 reports the node classification accuracy across eight benchmark datasets. HyperGRL demonstrates state-of-the-art (SOTA) performance, achieving the highest average accuracy (87.53 %) across all benchmarks, reflecting its superior generalization capability across diverse graph structures. Notably, HyperGRL achieves the highest accuracy on six out of the eight evaluated datasets (Cora, CiteSeer, PubMed, WikiCS, Amazon-Photo, and Coauthor-Physics), and delivers comparable or second-best results on the remaining two (Coauthor-CS and Amazon-Computers), with performance differences within 0.2% of the best model.

Compared to the supervised GCN baseline, HyperGRL demonstrates significant gains (e.g., 86.66 % vs 81.54 % on Cora), highlighting the strength of our self-supervised framework in exploiting structural information effectively without relying on labeled data. More importantly, HyperGRL establishes new SOTA results not only on smaller,

Table 2: Performance on node classification (Accuracy %) for supervised and unsupervised models. OOM indicates Out-Of-Memory on 24GB RTX 3090 GPU. Optimal results are shown in bold and suboptimal results are underlined. Avg. denotes the average accuracy computed across all eight datasets.

Model	Cora	CiteSeer	PubMed	WikiCS	Amz.-Comp.	Amz.-Photo	Co.-CS	Co.-Phy.	Avg.
MLP	47.92 \pm 0.41	49.31 \pm 0.26	69.14 \pm 0.34	71.98 \pm 0.42	73.81 \pm 0.21	78.53 \pm 0.32	90.37 \pm 0.19	93.58 \pm 0.41	71.83
GCN	81.54 \pm 0.68	70.73 \pm 0.65	79.16 \pm 0.25	77.19 \pm 0.12	86.51 \pm 0.54	92.42 \pm 0.22	93.03 \pm 0.31	95.65 \pm 0.16	84.53
DeepWalk	70.72 \pm 0.63	51.39 \pm 0.41	73.27 \pm 0.86	74.42 \pm 0.13	85.68 \pm 0.07	89.40 \pm 0.11	84.61 \pm 0.22	91.77 \pm 0.15	77.91
Node2Vec	71.08 \pm 0.91	47.34 \pm 0.84	66.23 \pm 0.95	71.76 \pm 0.14	84.41 \pm 0.14	89.68 \pm 0.19	85.16 \pm 0.04	91.23 \pm 0.07	75.61
DGI	82.24 \pm 0.63	71.82 \pm 0.61	76.80 \pm 0.30	75.42 \pm 0.17	84.05 \pm 0.42	91.62 \pm 0.37	92.14 \pm 0.55	94.54 \pm 0.52	83.83
GRACE	81.88 \pm 0.84	71.13 \pm 0.42	80.88 \pm 0.13	79.37 \pm 0.24	86.48 \pm 0.24	92.20 \pm 0.16	92.90 \pm 0.27	95.25 \pm 0.26	84.76
BGRL	81.86 \pm 0.32	72.10 \pm 0.31	80.65 \pm 0.42	79.28 \pm 0.45	89.21 \pm 0.47	92.28 \pm 0.44	92.73 \pm 0.41	95.31 \pm 0.26	85.68
VGAE	77.27 \pm 0.86	67.46 \pm 0.20	76.02 \pm 0.52	75.55 \pm 0.22	86.40 \pm 0.30	92.13 \pm 0.12	92.10 \pm 0.31	94.43 \pm 0.20	82.17
GMI	82.40 \pm 0.57	71.74 \pm 0.12	79.28 \pm 0.94	74.79 \pm 0.16	82.24 \pm 0.39	90.81 \pm 0.15	OOM	OOM	80.21
MVGRL	83.37 \pm 0.65	<u>73.29 \pm 0.36</u>	80.33 \pm 0.61	77.55 \pm 0.06	87.45 \pm 0.17	91.77 \pm 0.21	92.24 \pm 0.31	95.30 \pm 0.13	85.16
GCA	82.41 \pm 0.55	71.56 \pm 0.19	80.73 \pm 0.23	78.26 \pm 0.39	87.92 \pm 0.33	92.35 \pm 0.53	92.65 \pm 0.32	95.52 \pm 0.21	85.05
CCA-SSG	<u>84.17 \pm 0.44</u>	73.27 \pm 0.30	81.91 \pm 0.41	77.67 \pm 0.29	88.88 \pm 0.22	93.14 \pm 0.43	93.23 \pm 0.16	95.29 \pm 0.11	85.94
SUGRL	83.29 \pm 0.38	73.11 \pm 0.22	81.96 \pm 0.49	78.88 \pm 0.35	88.98 \pm 0.20	92.87 \pm 0.19	92.84 \pm 0.24	94.80 \pm 0.24	85.84
SGCL	82.17 \pm 0.16	69.50 \pm 0.82	79.98 \pm 0.31	<u>79.85 \pm 0.53</u>	90.70 \pm 0.30	93.46 \pm 0.30	93.29 \pm 0.17	95.78 \pm 0.11	85.34
SGRL	81.09 \pm 0.00	70.26 \pm 0.01	<u>86.56 \pm 0.19</u>	79.40 \pm 0.10	<u>90.23 \pm 0.03</u>	<u>93.95 \pm 0.03</u>	94.15 \pm 0.04	<u>96.23 \pm 0.01</u>	86.24
HyperGRL	86.66 \pm 0.14	74.65 \pm 0.16	86.89 \pm 0.05	81.88 \pm 0.15	89.68 \pm 0.10	94.24 \pm 0.02	<u>94.00 \pm 0.10</u>	96.25 \pm 0.05	87.53

low-homophily graphs like Cora and CiteSeer, but also on larger, dense, high-homophily graphs such as Amazon-Photo (94.24 %) and Coauthor-Physics (96.25 %). These widespread improvements verify that the proposed entropy-guided adaptive balancing effectively maintains a trade-off between local alignment and global uniformity, leading to stable and discriminative node representations.

5.3. Node Clustering

Table 3 reports the node clustering performance in terms of NMI across five benchmark datasets. HyperGRL demonstrates superior performance, achieving the highest average NMI of 0.6363, which surpasses the strongest baseline SGRL (0.6319) and consistently delivers competitive or superior results against all representative baselines (DGI, BGRL, and SGRL) across the individual datasets.

Specifically, HyperGRL attains the highest NMI on three datasets — Amazon-Computers (0.5526), Amazon-Photo (0.7155), and Coauthor-Physics (0.7272) — outperforming the second-best methods by 1.46%, 3.13%, and 0.40%, respectively. These consistent improvements demonstrate that our framework effectively enhances rep-

resentation separability, leading to more discriminative and semantically meaningful clusters, particularly on datasets with complex attribute distributions and dense relational patterns.

On the WikiCS dataset, HyperGRL achieves a suboptimal result to the best-performing DGI, ranking second with an NMI of 0.4239, only slightly lower than DGI’s 0.4312. A similar observation is made on Coauthor-CS, where SGRL and BGRL outperform our method. We attribute these minor gaps to the relatively homogeneous structural patterns of academic collaboration networks, where the advantages of hyperspherical dispersion and adaptive neighbor alignment are less prominent.

In summary, these results validate the effectiveness and generalization ability of HyperGRL in enhancing the clustering quality across diverse graph domains, particularly on datasets with rich feature diversity and complex topology.

Table 3: Performance on node clustering (NMI).

Dataset	DGI	BGRL	SGRL	HyperGRL
WikiCS	0.4312	0.3969	0.4188	<u>0.4239</u>
Amz.-Comp.	0.4630	0.5364	<u>0.5380</u>	0.5526
Amz.-Photo	0.5487	<u>0.6841</u>	0.6788	0.7155
Co.-CS	0.7162	<u>0.7732</u>	0.7961	0.7625
Co.-Phy.	0.6540	0.5568	<u>0.7232</u>	0.7272
Avg.	0.5626	0.5895	<u>0.6309</u>	0.6363

5.4. Link Prediction

Table 4 reports the link prediction results in terms of AUC across three benchmark datasets. Link prediction inherently requires structural reasoning, demanding that the model accurately capture topological similarities and latent connection patterns within the graph. HyperGRL consistently achieves strong and highly competitive results, obtaining the best AUC scores on Cora (98.10%) and CiteSeer (99.01%), while achieving comparable performance on PubMed (98.75%). Notably, on CiteSeer, HyperGRL surpasses the previous best model NCNC (97.65%) by more than 1.3%.

Table 4: Performance on link prediction (AUC).

Model	Cora	CiteSeer	PubMed	Avg.
Node2Vec	90.97 ± 0.64	94.46 ± 0.59	93.14 ± 0.18	92.86
MF	80.29 ± 2.26	75.92 ± 3.25	93.06 ± 0.43	83.09
MLP	95.32 ± 0.37	94.45 ± 0.32	98.34 ± 0.10	96.04
GCN	95.01 ± 0.32	95.89 ± 0.26	98.69 ± 0.06	96.53
GAT	93.90 ± 0.32	96.25 ± 0.20	98.20 ± 0.07	96.12
SAGE	95.63 ± 0.27	97.39 ± 0.15	98.87 ± 0.04	97.30
VGAE	95.08 ± 0.33	97.06 ± 0.22	97.47 ± 0.08	96.54
SEAL	90.59 ± 0.75	88.52 ± 1.40	97.77 ± 0.40	92.29
BUDDY	95.06 ± 0.36	96.72 ± 0.26	98.20 ± 0.05	96.66
Neo-GNN	93.73 ± 0.36	94.89 ± 0.60	98.71 ± 0.05	95.78
NCN	96.76 ± 0.18	97.04 ± 0.26	<u>98.98 ± 0.04</u>	97.59
NCNC	<u>96.90 ± 0.28</u>	<u>97.65 ± 0.30</u>	99.14 ± 0.03	<u>97.90</u>
NBFNet	92.85 ± 0.17	91.06 ± 0.15	98.34 ± 0.02	94.08
PEG	94.46 ± 0.34	96.15 ± 0.41	96.97 ± 0.39	95.86
HyperGRL	98.10 ± 0.40	99.01 ± 0.14	98.75 ± 0.08	98.62

In terms of overall performance, HyperGRL attains the highest average AUC of **98.62%**, outperforming the second-best method (NCNC, 97.90%) by a relative improvement of 0.74%. This high average score, combined with substantial improvements over both classical embedding methods (e.g., NODE2VEC, MF, MLP) and GNN-based baselines (GCN, GAT, SAGE, VGAE), highlights its ability to encode relational dependencies more effectively.

These consistent gains stem from the proposed joint optimization strategy, where the neighbor mean alignment reinforces local structural cohesion and the uniformity loss preserves global representational diversity, enabling accurate inference of latent node relations. The resulting model successfully generates high-quality node representations that are acutely sensitive to the underlying graph structure. Consequently, HyperGRL not only excels in feature-based node classification but also exhibits superior generalization in link prediction tasks that demand precise structural encoding.

5.5. Model Analysis

5.5.1. Ablation Studies

To evaluate the contribution of each objective component in HyperGRL, we conduct ablation studies on three benchmark datasets, with results summarized in Table 5. The full model consistently achieves the highest accuracy across all datasets, demonstrating the effectiveness of jointly optimizing the Neighbor-Mean Alignment loss and the Uniformity loss in an adversarial manner. Removing the alignment term $\mathcal{L}_{\text{align}}$ causes a noticeable performance drop, as the model fails to maintain local structural cohesion, leading to less coherent and less discriminative neighborhood representations. Notably, since GNNs inherently promote local consistency through message passing and aggregation, the degradation is moderate when $\mathcal{L}_{\text{align}}$ is omitted. In contrast, excluding the uniformity term $\mathcal{L}_{\text{unif}}$ results in a pronounced collapse of performance, where node embeddings exhibit over-smoothing and poor inter-class separability.

Overall, these results highlight the complementary roles of the two objectives: $\mathcal{L}_{\text{align}}$ enhances local structural consistency, while $\mathcal{L}_{\text{unif}}$ preserves global representational diversity—together enabling a well-balanced and highly discriminative embedding space.

Table 5: Ablation study on node classification (Accuracy %).

Variant	Cora	WikiCS	Co.-CS
Full model	86.66 ± 0.14	81.88 ± 0.15	94.00 ± 0.10
w/o $\mathcal{L}_{\text{align}}$	78.55 ± 0.34	81.12 ± 0.22	92.89 ± 0.39
w/o $\mathcal{L}_{\text{unif}}$	63.05 ± 0.54	49.65 ± 2.08	78.04 ± 0.56

5.5.2. Effect of Neighbor-Mean Alignment

To further examine the impact of the alignment target design, we compare the default HyperGRL, which adopts the Neighbor-Mean alignment strategy, with its variant HyperGRL-DN that replaces the neighbor mean with direct neighbor embeddings. As shown in Table 6, HyperGRL consistently achieves higher accuracy across all eight datasets, with especially notable improvements on Amazon-Computers (+1.15%)

Table 6: Effect of different alignment targets on node classification (Accuracy %). HyperGRL uses Neighbor-Mean Alignment, while HyperGRL-DN adopts Direct Neighbor Alignment (**DN**: Direct Neighbor variant).

Method	Cora	CiteSeer	PubMed	WikiCS	Amz.-Comp.	Amz.-Photo	Co.-CS	Co.-Phy.
HyperGRL	86.66 ± 0.14	74.65 ± 0.16	86.89 ± 0.05	81.88 ± 0.15	89.68 ± 0.10	94.24 ± 0.02	94.00 ± 0.10	96.25 ± 0.05
HyperGRL-DN	85.99 ± 0.25	74.05 ± 0.17	85.83 ± 0.14	81.25 ± 0.10	88.53 ± 0.18	93.45 ± 0.06	93.39 ± 0.19	95.57 ± 0.09

and PubMed (+1.06%). These results indicate that aggregating multi-hop neighbor information through the k -order mean provides a more stable and semantically coherent alignment target than individual neighbors. By smoothing local structural noise while preserving higher-order dependencies, the neighbor mean formulation enables the encoder to capture richer contextual patterns, ultimately yielding more discriminative and robust node representations.

5.5.3. Effect of Adaptive α

We further examine the effect of the entropy-guided adaptive balancing mechanism by comparing HyperGRL with fixed values of α against its adaptive variant. As shown in Figure 2, using a static α (e.g., 0.1, 0.5, or 1.0) leads to relatively stable convergence but limits performance due to the inability to dynamically balance alignment and uniformity across different training stages. In contrast, the adaptive α automatically adjusts its value according to the entropy-guided feedback, resulting in smoother optimization dynamics and more stable convergence behavior. More importantly, it consistently achieves the highest node classification accuracy, demonstrating that the entropy-guided balancing mechanism enables HyperGRL to maintain an appropriate trade-off between local alignment and global uniformity throughout training.

5.5.4. Effect of Backbone GNNs

We further examine the generality of our framework by substituting the default Transformer backbone with other widely used graph neural architectures, including GCN, GAT, and GraphSAGE. As shown in Table 7, the Transformer-based variant achieves the best overall performance, reaching 86.66% on Cora, 81.88% on WikiCS, and 94.00% on Coauthor-CS. While the other backbones yield slightly lower results, their accuracies remain comparable—around 86% on Cora, 81% on WikiCS, and 93–

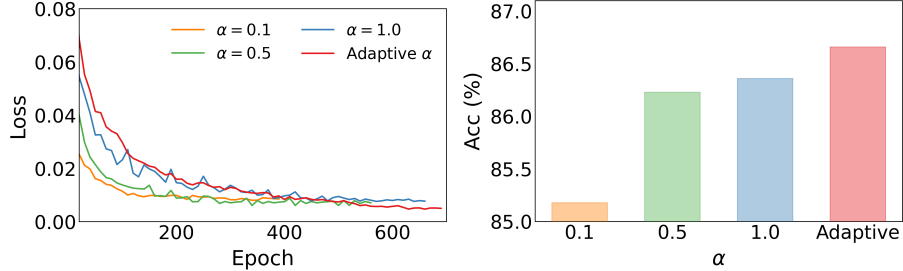


Figure 2: Effect of adaptive α .

94% on Coauthor-CS—demonstrating the robustness and consistency of our framework across different GNN architectures. These results highlight that HyperGRL not only adapts seamlessly to diverse backbone networks but also fully exploits the expressive power of Transformer architectures, achieving superior representation quality and stronger generalization across heterogeneous graph domains.

Table 7: Performance on node classification (Accuracy %) with different backbone networks.

Backbone	Cora	WikiCS	Co.-CS
GCN	85.78 ± 0.49	81.05 ± 0.06	93.57 ± 0.03
GAT	86.10 ± 0.23	80.90 ± 0.09	93.42 ± 0.08
GraphSAGE	85.87 ± 0.44	81.46 ± 0.10	93.71 ± 0.05
Transformer	86.66 ± 0.14	81.88 ± 0.15	94.00 ± 0.10

5.6. Hyperparameter Analysis

5.6.1. Impact of the target entropy H_{target}

To investigate the influence of the target entropy H_{target} , we fix all other hyperparameters and vary H_{target} from 1.5 to 5.0. As shown in Figure 3, both Cora and WikiCS exhibit relatively stable performance across a broad range of H_{target} values. Interestingly, even when H_{target} is set to a relatively low value, the model can still achieve superior accuracy. This indicates that the adaptive balancing mechanism dynamically adjusts the balance between alignment and uniformity during training, effectively compensating for suboptimal preset entropy targets. Therefore, HyperGRL does not require precise

manual tuning of H_{target} , demonstrating robustness and self-calibration capability across different entropy configurations.

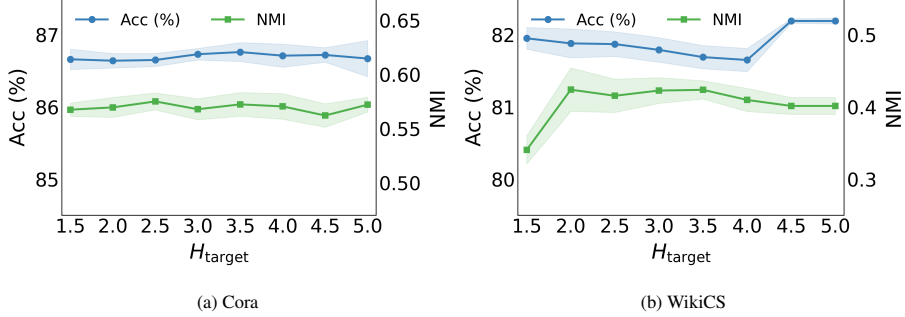


Figure 3: Impact of the target entropy H_{target} .

5.6.2. Impact of the neighbor-mean order k

To investigate the influence of the neighbor-mean order k , we fix all other hyperparameters and vary k from 1 to 3. As shown in Figure 4, increasing k generally enhances clustering performance, as a higher-order neighbor mean provides more consistent and globally aligned targets, leading to stronger structural cohesion among node embeddings. However, excessively large k values slightly reduce node classification accuracy, since the representations become overly smoothed and lose fine-grained, instance-specific characteristics that are crucial for discriminative classification. This observation suggests that moderate neighborhood aggregation achieves a favorable balance between alignment consistency and representation individuality.

5.6.3. Impact of Hidden Dimension

To investigate the effect of representation capacity, we vary the hidden dimension while keeping other hyperparameters fixed. Figure 5 compares the performance of SGCL, SGRL, and HyperGRL under different hidden dimensions on the Cora and WikiCS datasets. In both datasets, HyperGRL consistently outperforms the two baselines by a clear margin, demonstrating its superior ability to learn expressive and robust representations. As the hidden dimension increases, the performance of all methods gradually improves, suggesting that a larger embedding space enhances feature expressiveness.

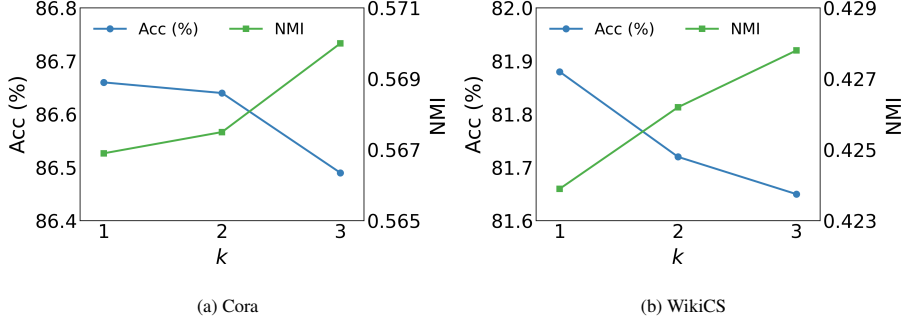


Figure 4: Impact of the neighbor-mean order k .

Notably, HyperGRL remains highly stable across different dimensions, maintaining competitive accuracy even in low-dimensional settings, which highlights its efficient utilization of representation capacity.

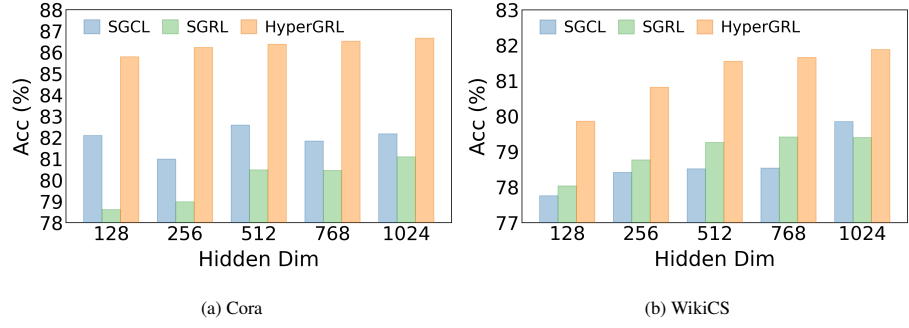


Figure 5: Performance on node classification (Accuracy %) with different hidden dimensions.

5.6.4. Impact of Network Depth

To examine the effect of network depth on representation propagation, we vary the number of GNN layers from 1 to 3 while keeping other hyperparameters unchanged. Figure 6 illustrates the results on the Cora and WikiCS datasets. Across both datasets, HyperGRL achieves the best accuracy and demonstrates remarkable robustness to changes in depth, whereas SGCL and SGRL exhibit noticeable performance fluctuations—particularly the sharp drop of SGRL with three layers. These findings indicate that deeper networks do not necessarily yield better performance, as excessive prop-

agation can cause over-smoothing and noise accumulation, which weaken feature discrimination. By contrast, HyperGRL effectively mitigates these issues through its alignment–uniformity regularization, preserving representation quality across different network depths.

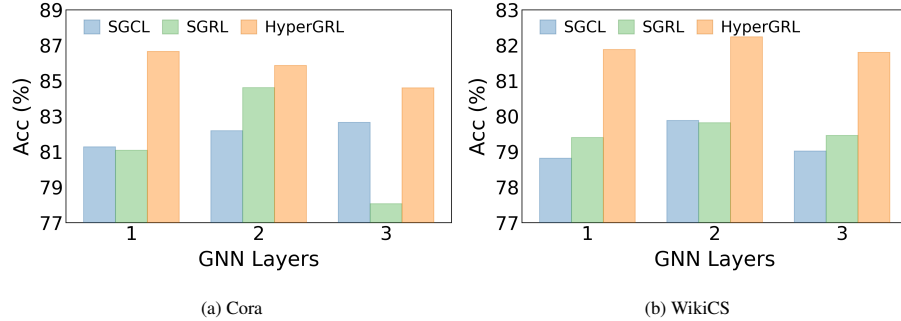


Figure 6: Performance on node classification (Accuracy %) with different network depths.

5.7. Visualization

To further illustrate the effectiveness of our approach, we visualize the learned node embeddings on the Cora dataset using t-SNE [44]. As shown in Figure 7, each point denotes a node and each color represents a class. The raw feature space (Figure 7(a)) exhibits substantial overlap between categories, indicating weak discriminative ability. With the uniformity-based method SGRL (Figure 7(b)), embeddings show improved clustering but still suffer from fuzzy category boundaries. The recent contrastive baseline SGCL (Figure 7(c)) achieves clearer separation, yet intra-class compactness and inter-class margins remain limited. In contrast, our proposed HyperGRL(Figure 7(d)) learns representations that form compact clusters within each class and simultaneously preserve distinct separation between different clusters of the same or different categories, yielding more discriminative and semantically aligned embeddings.

6. Conclusion

We introduce a novel framework that advances unsupervised graph representation learning by operationalizing the alignment–uniformity principle in a simple, principled, and robust manner. By leveraging neighbor-mean alignment to establish stable

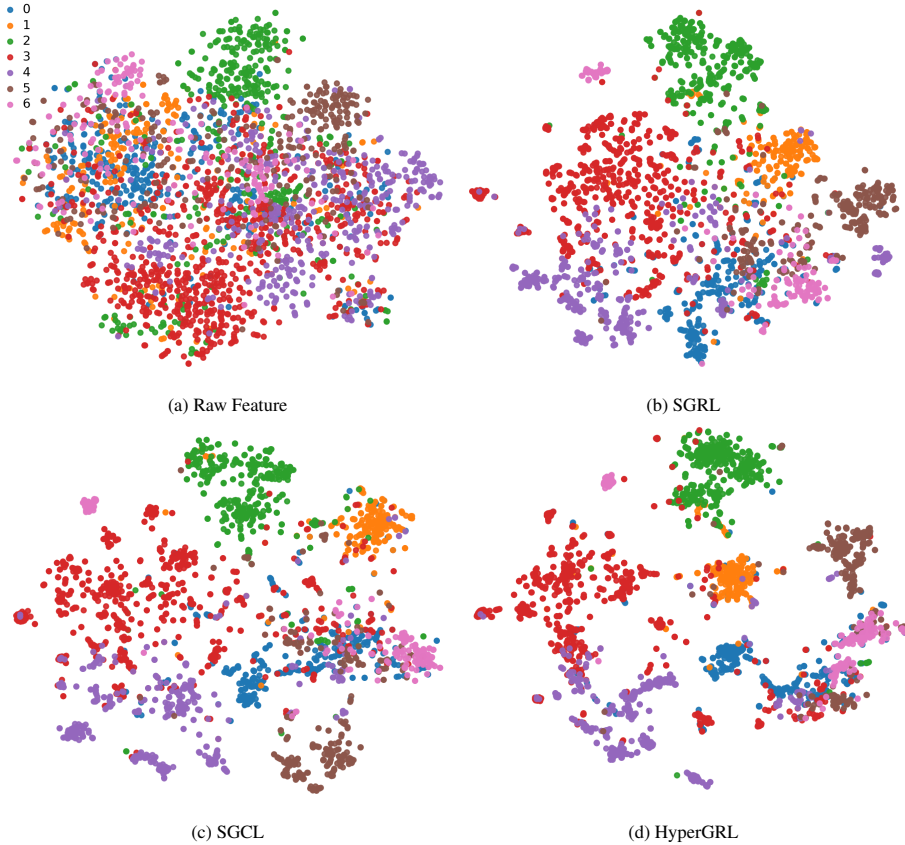


Figure 7: t-SNE embeddings of nodes in the Cora dataset. Each color represents a distinct class.

local cohesion without augmentations or auxiliary encoders, hyperspherical dispersion to enforce global uniformity sans negative sampling, and entropy-guided adaptive balancing to eliminate manual hyperparameter tuning, HyperGRL addresses key limitations of existing GRL methods, such as heuristic designs, computational overhead, and optimization instability. Our empirical evaluations across diverse benchmarks and downstream tasks—node classification, clustering, and link prediction—demonstrate that HyperGRL consistently outperforms state-of-the-art baselines in accuracy, stability, and generalizability, particularly on heterogeneous and large-scale graphs.

This work underscores the potential of geometrically grounded objectives to simplify and enhance self-supervised learning on graphs. However, the current formulation is

primarily validated on static graphs, leaving open questions regarding its efficiency and adaptability on dynamic graphs. Future extensions could incorporate temporal or multi-modal information, explore hierarchical or multi-view hyperspherical embeddings, and provide a more rigorous theoretical characterization of convergence and generalization properties. We believe that the proposed framework offers both methodological and conceptual insights that can benefit future research in geometric and self-supervised graph learning, and inspire broader applications in social networks, recommender systems, and biological graph modeling.

Declaration of competing interest

The authors declare that they have no known competing financial interests or personal relationships that could have appeared to influence the work reported in this paper.

Data availability

The datasets used in our experiments (Cora, CiteSeer, PubMed, WikiCS, Amazon-Computers, Amazon-Photo, Coauthor-CS, Coauthor-Physics) are publicly available benchmarks; relevant references are provided in the paper. Code and configurations are available at: <https://github.com/chenrui0127/HyperGRL>.

Acknowledgments

This work was supported by the National Natural Science Foundation of China (Nos. 62266028, 62266027, 62466029), the Key Projects of Basic Research in Yunnan Province (Nos. 202301AS070047, 202501AS070147), the Major Science and Technology Projects of Yunnan Province(Nos. 202502AD080016, 202402AD080002, 202402AG050007).

References

- [1] Y. Zhu, Y. Xu, F. Yu, Q. Liu, S. Wu, L. Wang, Deep graph contrastive representation learning, arXiv preprint arXiv:2006.04131 (2020).

- [2] P. Veličković, W. Fedus, W. L. Hamilton, P. Liò, Y. Bengio, R. D. Hjelm, Deep graph infomax, in: International Conference on Learning Representations, 2019.
- [3] S. Thakoor, C. Tallec, M. G. Azar, R. Munos, P. Veličković, M. Valko, Bootstrapped representation learning on graphs, in: ICLR 2021 Workshop on Geometrical and Topological Representation Learning, 2021.
- [4] A. v. d. Oord, Y. Li, O. Vinyals, Representation learning with contrastive predictive coding, arXiv preprint arXiv:1807.03748 (2018).
- [5] K. Hassani, A. H. Khasahmadi, Contrastive multi-view representation learning on graphs, in: International Conference on Machine Learning, Vol. 119, PMLR, 2020, pp. 4116–4126.
- [6] J.-B. Grill, F. Strub, F. Altché, C. Tallec, P. Richemond, E. Buchatskaya, C. Doersch, B. Avila Pires, Z. Guo, M. Gheshlaghi Azar, et al., Bootstrap your own latent-a new approach to self-supervised learning, *Adv. Neural Inf. Process. Syst.* 33 (2020) 21271–21284.
- [7] T. Wang, P. Isola, Understanding contrastive representation learning through alignment and uniformity on the hypersphere, in: International Conference on Machine Learning, PMLR, 2020, pp. 9929–9939.
- [8] Y. Zhu, Y. Xu, F. Yu, Q. Liu, S. Wu, L. Wang, Graph contrastive learning with adaptive augmentation, in: Proceedings of the Web Conference 2021, 2021, pp. 2069–2080.
- [9] J. Xia, L. Wu, G. Wang, J. Chen, S. Z. Li, Progcl: Rethinking hard negative mining in graph contrastive learning, in: International Conference on Machine Learning, Vol. 162, PMLR, 2022, pp. 24332–24346.
- [10] Y. Zheng, S. Pan, V. Lee, Y. Zheng, P. S. Yu, Rethinking and scaling up graph contrastive learning: An extremely efficient approach with group discrimination, *Adv. Neural Inf. Process. Syst.* 35 (2022) 10809–10820.

- [11] N. Lee, J. Lee, C. Park, Augmentation-free self-supervised learning on graphs, in: Proceedings of the AAAI Conference on Artificial Intelligence, Vol. 36, 2022, pp. 7372–7380.
- [12] W. Sun, J. Li, L. Chen, B. Wu, Y. Bian, Z. Zheng, Rethinking and simplifying bootstrapped graph latents, in: Proceedings of the 17th ACM International Conference on Web Search and Data Mining, 2024, pp. 665–673.
- [13] Y. You, T. Chen, Y. Sui, T. Chen, Z. Wang, Y. Shen, Graph contrastive learning with augmentations, *Adv. Neural Inf. Process. Syst.* 33 (2020) 5812–5823.
- [14] S. Thakoor, C. Tallec, M. G. Azar, M. Azabou, E. L. Dyer, R. Munos, P. Veličković, M. Valko, Large-scale representation learning on graphs via bootstrapping, in: International Conference on Learning Representations, 2022.
- [15] Y. Tian, C. Sun, B. Poole, D. Krishnan, C. Schmid, P. Isola, What makes for good views for contrastive learning?, *Adv. Neural Inf. Process. Syst.* 33 (2020) 6827–6839.
- [16] T. N. Kipf, M. Welling, Variational graph auto-encoders, arXiv preprint arXiv:1611.07308 (2016).
- [17] Z. Hou, X. Liu, Y. Cen, Y. Dong, H. Yang, C. Wang, J. Tang, Graphmae: Self-supervised masked graph autoencoders, in: Proceedings of the 28th ACM SIGKDD International Conference on Knowledge Discovery and Data Mining, 2022, pp. 594–604.
- [18] F.-Y. Sun, J. Hoffman, V. Verma, J. Tang, Infograph: Unsupervised and semi-supervised graph-level representation learning via mutual information maximization, in: International Conference on Learning Representations, 2020.
- [19] X. Wang, L. Peng, R. Hu, P. Hu, X. Zhu, Unsupervised multiplex graph representation learning via maximizing coding rate reduction, *Pattern Recognit.* 165 (2025) 111557.

- [20] Z. Luo, Y. Dong, Q. Zheng, H. Liu, M. Luo, Dual-channel graph contrastive learning for self-supervised graph-level representation learning, *Pattern Recognit.* 139 (2023) 109448.
- [21] J. Fang, S. Liang, Z. Meng, M. De Rijke, Hyperspherical variational co-embedding for attributed networks, *ACM Trans. Inf. Syst.* 40 (3) (2021) 1–36.
- [22] P. Wang, D. Wu, C. Chen, K. Liu, Y. Fu, J. Huang, Y. Zhou, J. Zhan, X. Hua, Deep adaptive graph clustering via von mises-fisher distributions, *ACM Trans. Web* 18 (2) (2024) 1–21.
- [23] J. Lu, D. Wu, F. Nie, R. Wang, X. Li, Hyperspherical prototype node clustering, *Trans. Mach. Learn. Res.* (2024).
- [24] D. He, L. Shan, J. Zhao, H. Zhang, Z. Wang, W. Zhang, Exploitation of a latent mechanism in graph contrastive learning: Representation scattering, *Adv. Neural Inf. Process. Syst.* 37 (2024) 115351–115376.
- [25] S. Yun, M. Jeong, R. Kim, J. Kang, H. J. Kim, Graph transformer networks, *Adv. Neural Inf. Process. Syst.* 32 (2019).
- [26] T. N. Kipf, M. Welling, Semi-supervised classification with graph convolutional networks, in: *International Conference on Learning Representations*, 2017.
- [27] P. Veličković, G. Cucurull, A. Casanova, A. Romero, P. Lio, Y. Bengio, Graph attention networks, in: *International Conference on Learning Representations*, 2018.
- [28] W. Hamilton, Z. Ying, J. Leskovec, Inductive representation learning on large graphs, *Adv. Neural Inf. Process. Syst.* 30 (2017).
- [29] P. Mernyei, C. Cangea, Wiki-cs: A wikipedia-based benchmark for graph neural networks, *arXiv preprint arXiv:2007.02901* (2020).
- [30] O. Shchur, M. Mumme, A. Bojchevski, S. Günnemann, Pitfalls of graph neural network evaluation, *arXiv preprint arXiv:1811.05868* (2018).

- [31] B. Perozzi, R. Al-Rfou, S. Skiena, Deepwalk: Online learning of social representations, in: Proceedings of the 20th ACM SIGKDD International Conference on Knowledge Discovery and Data Mining, 2014, pp. 701–710.
- [32] A. Grover, J. Leskovec, Node2vec: Scalable feature learning for networks, in: Proceedings of the 22nd ACM SIGKDD International Conference on Knowledge Discovery and Data Mining, 2016, pp. 855–864.
- [33] Z. Peng, W. Huang, M. Luo, Q. Zheng, Y. Rong, T. Xu, J. Huang, Graph representation learning via graphical mutual information maximization, in: Proceedings of the Web Conference 2020, 2020, pp. 259–270.
- [34] H. Zhang, Q. Wu, J. Yan, D. Wipf, P. S. Yu, From canonical correlation analysis to self-supervised graph neural networks, *Adv. Neural Inf. Process. Syst.* 34 (2021) 76–89.
- [35] Y. Mo, L. Peng, J. Xu, X. Shi, X. Zhu, Simple unsupervised graph representation learning, in: Proceedings of the AAAI Conference on Artificial Intelligence, Vol. 36, 2022, pp. 7797–7805.
- [36] A. K. Menon, C. Elkan, Link prediction via matrix factorization, in: Joint European Conference on Machine Learning and Knowledge Discovery in Databases, Springer, 2011, pp. 437–452.
- [37] M. Zhang, Y. Chen, Link prediction based on graph neural networks, *Adv. Neural Inf. Process. Syst.* 31 (2018).
- [38] B. P. Chamberlain, S. Shirobokov, E. Rossi, F. Frasca, T. Markovich, N. Y. Hammerla, M. M. Bronstein, M. Hansmire, Graph neural networks for link prediction with subgraph sketching, in: International Conference on Learning Representations, 2023.
- [39] Z. Zhu, Z. Zhang, L.-P. Khonneux, J. Tang, Neural bellman-ford networks: A general graph neural network framework for link prediction, *Adv. Neural Inf. Process. Syst.* 34 (2021) 29476–29490.

- [40] S. Yun, S. Kim, J. Lee, J. Kang, H. J. Kim, Neo-gnns: Neighborhood overlap-aware graph neural networks for link prediction, *Adv. Neural Inf. Process. Syst.* 34 (2021) 13683–13694.
- [41] H. Wang, H. Yin, M. Zhang, P. Li, Equivariant and stable positional encoding for more powerful graph neural networks, in: *International Conference on Learning Representations*, 2022.
- [42] X. Wang, H. Yang, M. Zhang, Neural common neighbor with completion for link prediction, in: *International Conference on Learning Representations*, 2024.
- [43] J. Li, H. Shomer, H. Mao, S. Zeng, Y. Ma, N. Shah, J. Tang, D. Yin, Evaluating graph neural networks for link prediction: Current pitfalls and new benchmarking, *Adv. Neural Inf. Process. Syst.* 36 (2023) 3853–3866.
- [44] L. v. d. Maaten, G. Hinton, Visualizing data using t-sne, *J. Mach. Learn. Res.* 9 (2008) 2579–2605.